

Computational and electrochemical studies of some amino acid compounds as corrosion inhibitors for mild steel in hydrochloric acid solution

Jia-jun Fu · Su-ning Li · Ying Wang ·
Lin-hua Cao · Lu-de Lu

Received: 29 April 2010 / Accepted: 14 June 2010 / Published online: 26 June 2010
© Springer Science+Business Media, LLC 2010

Abstract The corrosion inhibition behaviour of four selected amino acid compounds, namely L-cysteine, L-histidine, L-tryptophan and L-serine on mild steel surface in deaerated 1 M HCl solution were studied electrochemically by Tafel polarization and electrochemical impedance spectroscopy methods and computationally by the quantum chemical calculation and molecular dynamics simulation. Electrochemical results show that these amino acid compounds inhibit the corrosion of mild steel in 1 M HCl solution significantly. The order of inhibition efficiency of these inhibitors follows the sequence: L-tryptophan > L-histidine > L-cysteine > L-serine. The quantum chemical calculations were performed to characterize the electronic parameters which are associated with inhibition efficiency. The molecular dynamics simulations were applied to find the equilibrium adsorption configurations and calculate the interaction energy between inhibitors and iron surface. Results obtained from Tafel and impedance methods are in good agreement. The electrochemical experimental results are supported by the theoretical data.

Introduction

The use of corrosion inhibitors is one of the most effective and economic methods to protect metal surfaces against corrosion in aggressive media [1–3]. Most of the efficient pickling inhibitors are organic compounds that contain mainly nitrogen, oxygen, sulphur phosphorus, and multiple bonds or aromatic rings in their structures. The number of

lone pairs of electrons and loosely bound π -electrons in these functional groups are the key structural features that determine the inhibition efficiency [4, 5]. However, the toxicity of these compounds is also documented [6]. Environmental restrictions imposed on heavy-metal and phosphonate-based corrosion inhibitors, guided scientific researches towards studying non-toxic and non-phosphorus environmental-friendly corrosion inhibitors [7–9].

Amino acids are non-toxic, relatively cheap, and easy to produce with purities greater than 99%. They are considered to be more promising green inhibitors [10]. Amino acid compounds were reported to show corrosion resistant behaviour on copper, mild steel and aluminium alloy [11–17]. In the previous literature, most attention was paid to the mechanism of adsorption and also to the relationship between the structure of inhibitors, their adsorption on the metal surface, and their inhibition efficiencies on the macroscopic level. With the in-depth study of organic corrosion inhibitors, it has been found that the inhibition efficiency depends on some physicochemical properties of inhibitors, such as functional groups, steric effects, electronic density at the donor atom, π orbital character and corrosive environment [18–21]. Therefore, theoretical prediction of the efficiency of corrosion inhibitors has become very popular [22–25]. Quantum chemical calculation and molecular dynamic simulation have become an effective way to study the correlation between molecular structure and inhibition properties on the microcosmic level. Quantum chemical calculations have proved to be a very powerful tool for studying corrosion inhibition mechanism and helped to design the novel high efficiency inhibitors by the quantitative structure–activity relationship (QSAR) method [26–28]. Molecular dynamic simulation is used as a beneficial supplement of quantum chemical method, which is applied to study the interaction between

J. Fu (✉) · S. Li · Y. Wang · L. Cao · L. Lu
School of Chemical Engineering, Nanjing University of Science and Technology, Nanjing 210094, JiangSu, China
e-mail: fujiajun668@gmail.com

inhibitors and metal surface. This provides a convenient way to study the complex system, which includes one inhibitor molecule, hundreds of solvent molecules and the metal surface. It also solves the problem that quantum chemical method is usually used for small systems containing between 10 and 100 atoms [29–32]. Due to expensive and time-consuming of experimental methods, it can be inferred that these two theoretical methods will play more and more important role in studying corrosion inhibitors with the continuous development of computer hardware and software technology.

The purpose of this paper is to evaluate L-cysteine (L-Cys), L-histidine (L-His), L-tryptophan (L-Try) and L-serine (L-Ser) as corrosion inhibitor for mild steel in 1 M deaerated HCl solution by potentiodynamic polarization and electrochemical impedance spectroscopy (EIS) techniques. Another objective in this work is to discuss the relationship between quantum chemical parameters, such as the highest occupied molecular orbital (E_{HOMO}), lowest unoccupied molecular orbital (E_{LUMO}), the energy gap (ΔE , $\Delta E = E_{\text{LUMO}} - E_{\text{HOMO}}$), dipole moment (μ) and the experimental inhibition efficiencies. Furthermore, the adsorption characteristics of these amino acid compounds on the iron surface using molecular dynamics simulations were also performed.

Experimental

Materials

L-Cys, L-His, L-Try and L-Ser were purchased from Acros Organics. The chemical structures, names and abbreviations of amino acid compounds were given in Table 1. The 1 M HCl solution was made with AR grade HCl and double distilled water. The composition of mild steel used in the experiments was shown in Table 2. The working electrode (WE) was in the form of a rod machined into a cylindrical form embedded in epoxy resin leaving an open surface area of 1 cm². The exposed surface was abraded with emery paper (from grade #600 to #2000), rinsed by double distilled water, degreased with acetone, dried at room temperature before electrochemical use.

Electrochemical measurements

Electrochemical measurements were performed in a conventional three-electrode cell of capacity 500 mL. The WE, a reference saturated calomel electrode (SCE) and platinum counter electrode were placed inside a three-electrode cell. The HCl solution was degreased with ultra-pure nitrogen bubbling for 30 min to avoid any reactions with dissolved oxygen. Measurements were performed at

Table 1 The chemical structures, names and abbreviations of the compounds

| Chemical structure | Name | Abbreviation |
|--------------------|--------------|--------------|
| | L-Cysteine | L-Cys |
| | L-Histidine | L-His |
| | L-Tryptophan | L-Try |
| | L-Serine | L-Ser |

Table 2 The chemical composition (wt%) of mild steel sample

| Composition | C | Mn | P | S | Fe |
|-------------|------|------|------|------|------|
| Weight (%) | 0.18 | 0.64 | 0.05 | 0.06 | Bal. |

room temperature, 25 °C with PARSTAT 2273 (Princeton Applied Research Company). The WE was immersed in 1 M HCl solution for 30 min until a steady-state open circuit potential (OCP) was obtained. Tafel polarization scans were carried out by changing the electrode potential automatically from –250 to +250 mV versus OCP with a scan rate of 0.166 mV/s. The data recordings and the calculation of the electrochemical parameters were performed using PowerSuite software. EIS were carried out at OCP over a frequency range of 100 kHz–10 MHz. The sinusoidal potential perturbation was 5 mV in amplitude. The data were collected using PowerSuite software and

interpreted with Zsimpwin software. Each test was run in triplicate to verify the reproducibility and the average values reported. All potentials were referred to the SCE.

Quantum chemistry calculations

The amino acid compounds have been fully optimized at the using B3LYP Density Functional Theory (DFT) with 6-311G(d,p) basis set with Gaussian 03W program. This basis set provided accurate geometry and electronic properties for a wide range of organic compounds. The following quantum chemical parameters, which indicate structural characteristics of these inhibitors, were considered: E_{HOMO} , E_{LUMO} , ΔE and μ .

DFT has also been found to be successful in providing insights into the chemical reactivity and selectivity, in terms of global parameters such as electronegativity (χ), hardness (η) and local ones such as the Fukui function ($f(\vec{r})$). The local reactivity of the molecules was analyzed through an evaluation of the Fukui indices. These are a measurement of the chemical reactivity, as well as an

indicative of the reactive regions and the nucleophilic and electrophilic behaviour of the molecule. The Fukui function $f(\vec{r})$ is defined as the derivative of the electronic density $\rho(\vec{r})$ with respect to the number of electrons N at a constant external potential $v(\vec{r})$ [33]:

$$f(\vec{r}) = (\partial \rho(\vec{r}) / \partial N)_{f(\vec{r})} \quad (1)$$

If the effects of relaxation associated with the addition or removal of electronic charges are not considered, then

$$\rho^+(\vec{r}) \approx \rho_{\text{LUMO}}(\vec{r}) \quad (2)$$

$$\rho^-(\vec{r}) \approx \rho_{\text{HOMO}}(\vec{r}) \quad (3)$$

where $\rho_{\text{LUMO}}(\vec{r})$ is the density of the first unoccupied molecular orbital and $\rho_{\text{HOMO}}(\vec{r})$ is the density of the highest occupied molecular orbital.

The condensed Fukui function calculations are based on the finite difference approximations and partitioning of the electron density $\rho(\vec{r})$ between atoms in a molecular system.

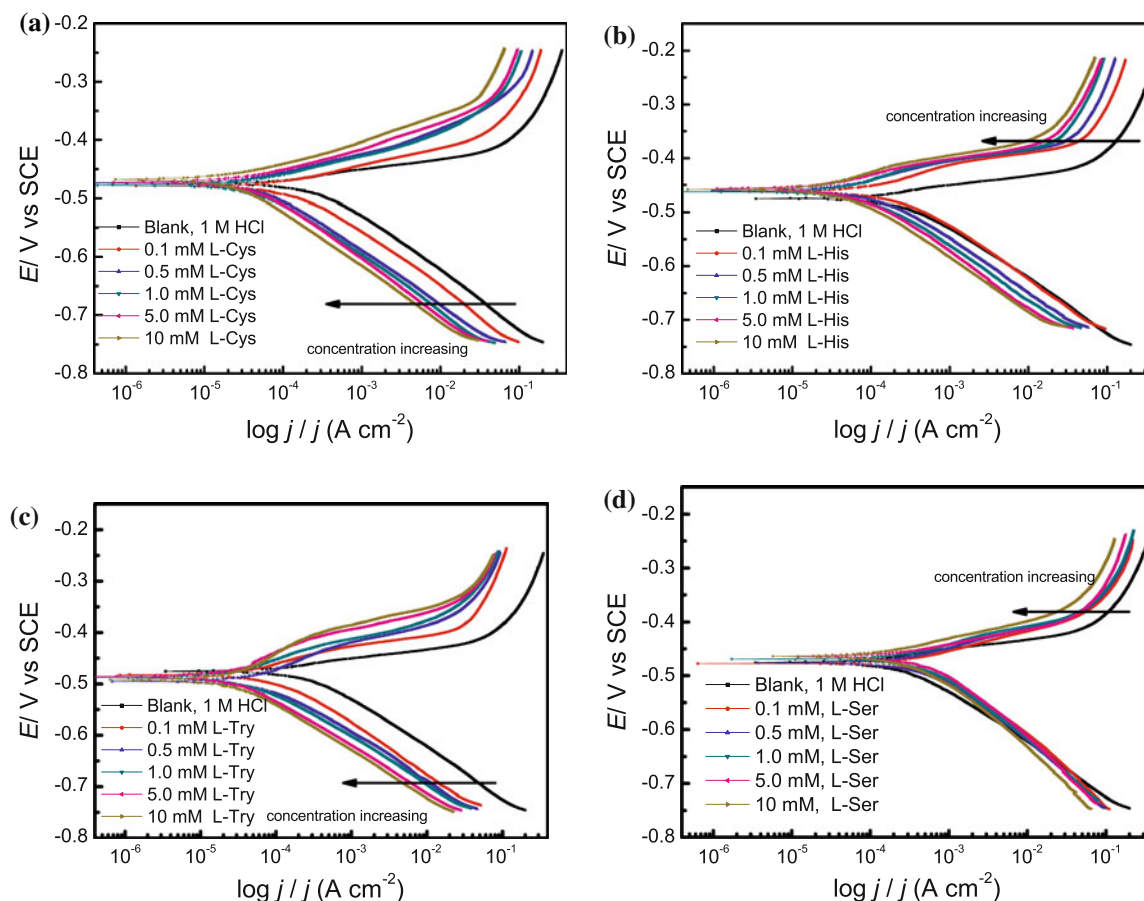


Fig. 1 The anodic and cathodic polarization curves in 1 M HCl in the absence and presence of various concentration of **a** L-Cys, **b** L-His, **c** L-Try, **d** L-Ser

$$f_k^+ = q_k(N+1) - q_k(N) \quad (\text{for nucleophilic attack}) \quad (4)$$

$$f_k^- = q_k(N) - q_k(N-1) \quad (\text{for electrophilic attack}) \quad (5)$$

$$f_k^0 = \frac{q_k(N+1) - q_k(N-1)}{2} \quad (\text{for radial attack}) \quad (6)$$

where q_k is the gross charge of atom k in the molecule and N is the number of electrons. The condensed Fukui function is local reactivity descriptor and can be used only for comparing reactive atomic centres within the same molecule [34].

The Fukui function calculations were performed with DMol³ version 4.3 available in Material Studio software (Accelrys, San Diego, CA), using a PBE (Perdew, Burke and Enzerhof) functional and a double-numeric quality basis set with polarization functions (DND). Dmol³ use a Mulliken population analysis.

Molecular dynamics simulations

The molecular dynamics simulations were performed using the software, Material Studio 4.3. As to the three kinds of Fe surface (1 1 0, 1 0 0, 1 1 1), Fe (1 1 1) and Fe (1 0 0) surfaces have relatively open structures whereas Fe (1 1 0) is a densely packed surface and has the most stabilization.

Therefore, the surface of Fe (1 1 0) was chosen to simulate the adsorption process. The molecular dynamics simulation of the interaction between the inhibitor molecule dissolved in H₂O and the Fe (1 1 0) surface was carried out in a simulation box (32.3 Å × 32.3 Å × 30.9 Å) with periodic boundary conditions in order to simulate a representative part of an interface devoid of any arbitrary boundary effects. The inhibitor molecule was energy optimized, Fe (1 1 0) surface and water layers was constructed using the amorphous cell module. The molecular dynamics simulation was performed under 25 °C, NVT ensemble, with a time step of 0.1 fs and simulation time of 50 ps. Details of simulation process can be referred to some previous literature [35, 36].

The interaction energy $E_{\text{Fe-inhibitor}}$ of iron surface with the inhibitor was calculated according to the following equation:

$$E_{\text{Fe-inhibitor}} = E_{\text{Complex}} - (E_{\text{Fe}} + E_{\text{Inhibitor}}) \quad (7)$$

where E_{complex} is the total energy of the Fe crystal together with the adsorbed inhibitor molecule, E_{Fe} and $E_{\text{Inhibitor}}$ is the total energy of the iron crystal and free inhibitor molecule, respectively. And the binding energy is the negative value of the interaction energy, $E_{\text{binding}} = -E_{\text{Fe-inhibitor}}$.

Table 3 Electrochemical kinetic parameters obtained by Tafel polarization technology for mild steel in 1 M HCl without and with various concentrations of L-Cys, L-His, L-Try and L-Ser at 25 °C

| Inhibitor | C_{inh} (mol L ⁻¹) | E_{corr} vs. SCE (mV) | j_{corr} (μA cm ⁻²) | $-\beta_c$ (mV dec ⁻¹) | β_a (mV dec ⁻¹) | IE_p (%) | θ (%) |
|-----------|---|--------------------------------|--|------------------------------------|-----------------------------------|------------|--------------|
| Blank | – | –475 | 485 | 85.6 | 28.4 | – | – |
| L-Cys | 1×10^{-4} | –479 | 293 | 90.1 | 35.8 | 39.5 | 0.395 |
| | 5×10^{-4} | –473 | 215 | 88.1 | 39.3 | 55.6 | 0.556 |
| | 1×10^{-3} | –478 | 172 | 88.2 | 37.4 | 64.5 | 0.645 |
| | 5×10^{-3} | –472 | 125 | 96.2 | 42.6 | 74.1 | 0.741 |
| | 1×10^{-2} | –467 | 72 | 93.5 | 42.1 | 85.1 | 0.851 |
| | 1×10^{-4} | –462 | 230 | 89.1 | 44.2 | 52.5 | 0.525 |
| L-His | 5×10^{-4} | –460 | 184 | 92.7 | 50.1 | 62.1 | 0.621 |
| | 1×10^{-3} | –462 | 110 | 81.2 | 54.1 | 77.2 | 0.772 |
| | 5×10^{-3} | –456 | 61 | 84.3 | 63.5 | 87.5 | 0.875 |
| | 1×10^{-2} | –458 | 32 | 93.1 | 57.4 | 93.4 | 0.934 |
| | 1×10^{-4} | –477 | 157 | 93.7 | 33.5 | 67.5 | 0.675 |
| L-Try | 5×10^{-4} | –476 | 72 | 87.9 | 35.6 | 85.2 | 0.852 |
| | 1×10^{-3} | –468 | 37 | 95.8 | 31.2 | 92.3 | 0.923 |
| | 5×10^{-3} | –464 | 22 | 94.8 | 35.5 | 95.5 | 0.955 |
| | 1×10^{-2} | –463 | 18 | 92.4 | 36.1 | 96.3 | 0.963 |
| | 1×10^{-4} | –495 | 509 | 82.1 | 49.1 | –5.12 | –0.051 |
| L-Ser | 5×10^{-4} | –482 | 436 | 79.2 | 47.3 | 10.2 | 0.102 |
| | 1×10^{-3} | –486 | 376 | 78.5 | 42.9 | 22.4 | 0.224 |
| | 5×10^{-3} | –486 | 319 | 85.9 | 44.1 | 34.2 | 0.342 |
| | 1×10^{-2} | –491 | 283 | 87.1 | 46.3 | 41.5 | 0.415 |

Results and discussions

Tafel polarization studies

Figure 1 show the cathodic and anodic polarization curves of the mild steel immersed in 1 M HCl at 25 °C in absence and presence of various concentrations of L-Cys, L-His, L-Try and L-Ser, respectively. Electrochemical parameters such as corrosion potentials (E_{corr}), anodic and cathodic Tafel slopes (β_a and β_c), corrosion current densities (j_{corr}), percentage inhibition efficiencies (IE_p , %), and degrees of surface coverage (θ), for various concentrations of these amino acid compounds were given in Table 3. The percentage inhibition efficiency and the degree of surface coverage were calculated using the following formulas:

$$IE_p(\%) = \left(\frac{j_0 - j_1}{j_0} \right) \times 100 \quad (8)$$

$$\theta = \frac{j_0 - j_1}{j_0} \quad (9)$$

where j_0 and j_1 are the corrosion current densities for without and with inhibitors, respectively.

From the results in Table 3, it can be easily seen that these four amino acid compounds under investigation conditions are efficient inhibitors. It is also found that j_{corr} values decreased considerably in presence of inhibitors and decreased with increasing inhibitor concentration except for L-Ser with the concentration of 1.0×10^{-4} mol L⁻¹. In this case, the stimulating effect on corrosion process was stronger than the suppression effect [37]. By comparing the j_{corr} in Table 3, the inhibition efficiency of these four amino acid compounds decreases in the order: L-Try > L-His > L-Cys > L-Ser under the same conditions. L-Try shows the maximum inhibition efficiency among all the other investigated compounds at the concentration of 1.0×10^{-2} mol L⁻¹.

As seen from Fig. 1, the anodic and cathodic polarization curves were inhibited after the addition of four amino acid compounds. This means that the addition of the investigated inhibitors not only reduce anodic dissolution but also retard the hydrogen evolution reaction. The unchanged anodic and cathodic Tafel slopes indicated that the four compounds act as adsorptive inhibitors, suppressing both anodic and cathodic reaction by adsorbing on mild steel surface and blocking the active sites [21].

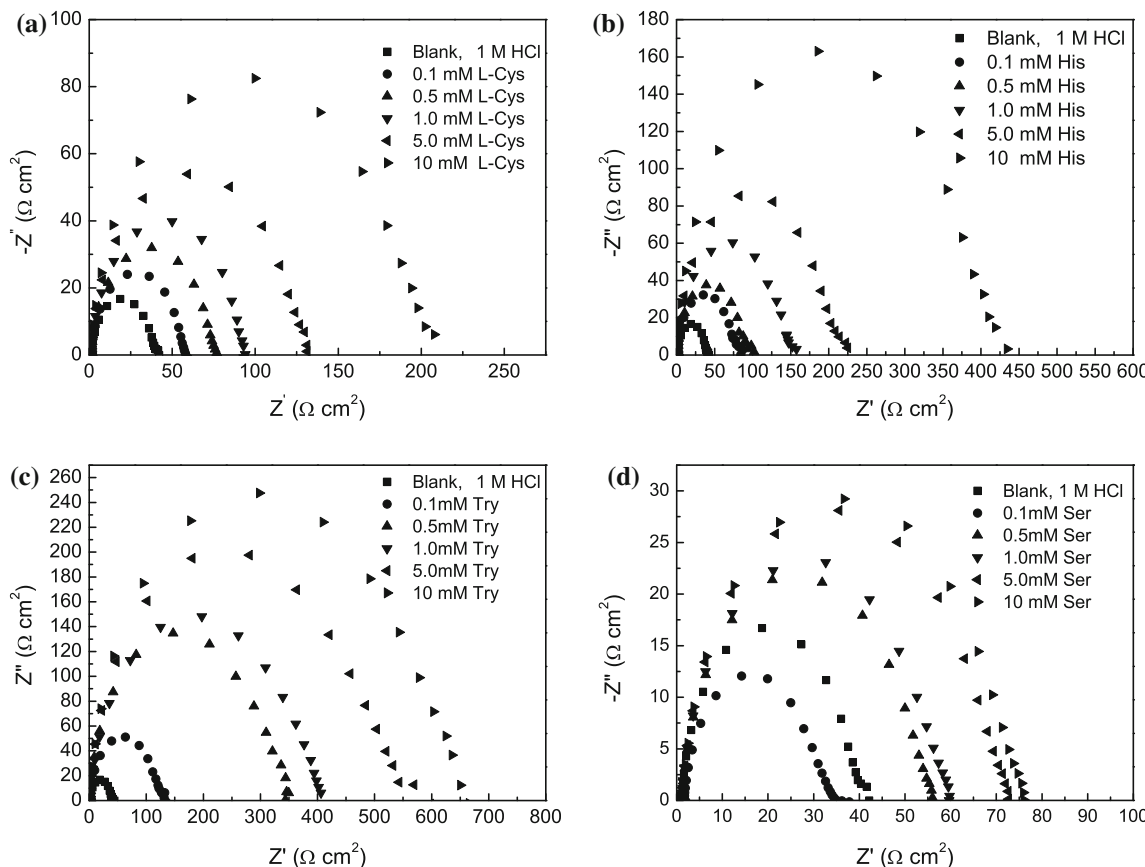


Fig. 2 Impedance plot of mild steel obtained in 1M HCl in the absence and presence of various concentration of **a** L-Cys, **b** L-His, **c** L-Try, **d** L-Ser

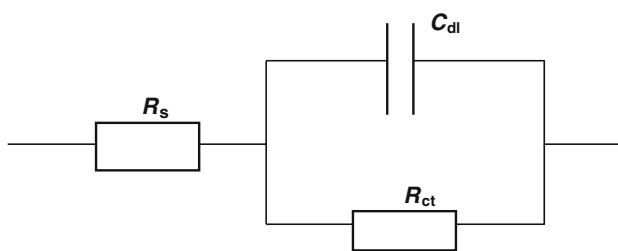


Fig. 3 Equivalent circuit model for impedance analysis

Furthermore, E_{corr} shifted slightly (<30 mV) in all cases. Based on these experimental results, the four amino acid compounds can be regarded as mixed-type inhibitors [38]. However, the changing trends of E_{corr} for four inhibitors are not the same. No definite trend was observed in the shift of E_{corr} values, in the presence of various concentrations of L-Cys and L-Ser. But for L-His and L-Try, the E_{corr} shifted slightly in the positive direction with increase in L-His concentration, while E_{corr} shifted slightly in the negative direction with increase in L-Try concentration. Therefore, it can be inferred that L-Try acts more as a cathodic than anodic inhibitor, and in the contrary, L-His acts more as an anodic inhibitor than cathodic inhibitor.

Electrochemical impedance spectroscopy studies

Nyquist plots for mild steel in 1 M HCl in the absence and presence of the four amino acid compounds in the concentration range of 1.0×10^{-4} – 1.0×10^{-2} mol L $^{-1}$ at 25 °C were shown in Fig. 2. It is apparent from this figure that all Nyquist plots are similar in shape and consist of a single capacitive loop, which mean only one charge transfer reaction during metal dissolution process [39]. The simple equivalent circuit model for this system is shown in Fig. 3. The circuit comprises a solution resistance R_s , in series with the parallel combination of the charge transfer resistance R_{ct} and a double layer capacitance (C_{dl}). C_{dl} values were calculated from the frequency at which the imaginary component of impedance was maximum using the following equation:

$$C_{\text{dl}} = \frac{1}{2\pi f_{\max} R_{\text{ct}}} \quad (10)$$

where f_{\max} is the frequency at which the imaginary component of impedance is maximum.

The impedance diagram does not give a perfect semi-circle, which has been attributed to frequency dispersion of interfacial impedance. The percentage Inhibition efficiency (IE_E , %) can be calculated as following equation:

$$IE_E(\%) = \frac{R_{\text{ct}} - R_{\text{ct}}^0}{R_{\text{ct}}} \times 100 \quad (11)$$

where R_{ct} and R_{ct}^0 are the polarization resistance of mild steel with and without inhibitor molecules. Inhibition efficiencies and the impedance parameters derived from Nyquist plots are given in Table 4. The charge transfer resistance R_{ct} values increased and the capacitance values C_{dl} decreased with increasing concentration of four amino acid compounds. The increase in R_{ct} is attributed to the formation of protective film on the metal/solution interface. The decrease in C_{dl} can be interpreted as a decrease in local dielectric constant and/or an increase in the thickness of electronic double layer, which result from the adsorption of the amino acid molecules on the metal surface [40]. It can be seen that the IE_E values obtained from the EIS are in complete agreement with those obtained from Tafel polarization measurements.

Quantum chemistry calculation

To investigate the relationship between the molecular electronic structure of inhibitors and their inhibition efficiencies, quantum chemical calculations were performed. The optimized structures of the four amino acid compounds were shown in Fig. 4. Quantum chemical parameters such as E_{HOMO} , E_{LUMO} , ΔE and μ were given in

Table 4 Electrochemical impedance parameters and the corresponding inhibition efficiencies for mild steel in 1 M HCl solution in the absence and presence of different concentrations of inhibitors at 25 °C

| Inhibitors | C_{inh} (mol L $^{-1}$) | R_{ct} (Ω cm 2) | C_{dl} ($\mu\text{F cm}^{-2}$) | IE_E (%) |
|------------|-----------------------------------|--------------------------------------|---|------------|
| Blank | 0 | 36.71 | 169.4 | – |
| L-Cys | 1×10^{-4} | 54.13 | 133.2 | 32.18 |
| | 5×10^{-4} | 74.18 | 72.48 | 50.51 |
| | 1×10^{-3} | 88.04 | 102.2 | 58.30 |
| | 5×10^{-3} | 111.3 | 93.9 | 67.01 |
| | 1×10^{-2} | 188.2 | 81.94 | 80.49 |
| | 1×10^{-4} | 73.14 | 151.2 | 49.80 |
| L-His | 5×10^{-4} | 95.36 | 125.6 | 61.50 |
| | 1×10^{-3} | 138.4 | 113.8 | 73.47 |
| | 5×10^{-3} | 194.4 | 104.4 | 81.12 |
| | 1×10^{-2} | 379.9 | 75.54 | 90.34 |
| | 1×10^{-4} | 118.4 | 133 | 68.99 |
| | 5×10^{-4} | 322 | 98.55 | 88.60 |
| L-Try | 1×10^{-3} | 496.5 | 87.4 | 92.60 |
| | 5×10^{-3} | 500.8 | 44.29 | 92.67 |
| | 1×10^{-2} | 617.8 | 40.57 | 94.06 |
| | 1×10^{-4} | 29.85 | 155.52 | –22.98 |
| | 5×10^{-4} | 52.44 | 156.91 | 29.96 |
| | 1×10^{-3} | 54.93 | 146.19 | 33.17 |
| L-Ser | 5×10^{-3} | 67.21 | 135.29 | 45.38 |
| | 1×10^{-2} | 70.05 | 114.19 | 47.59 |

Fig. 4 Optimized structures of four amino acid compounds

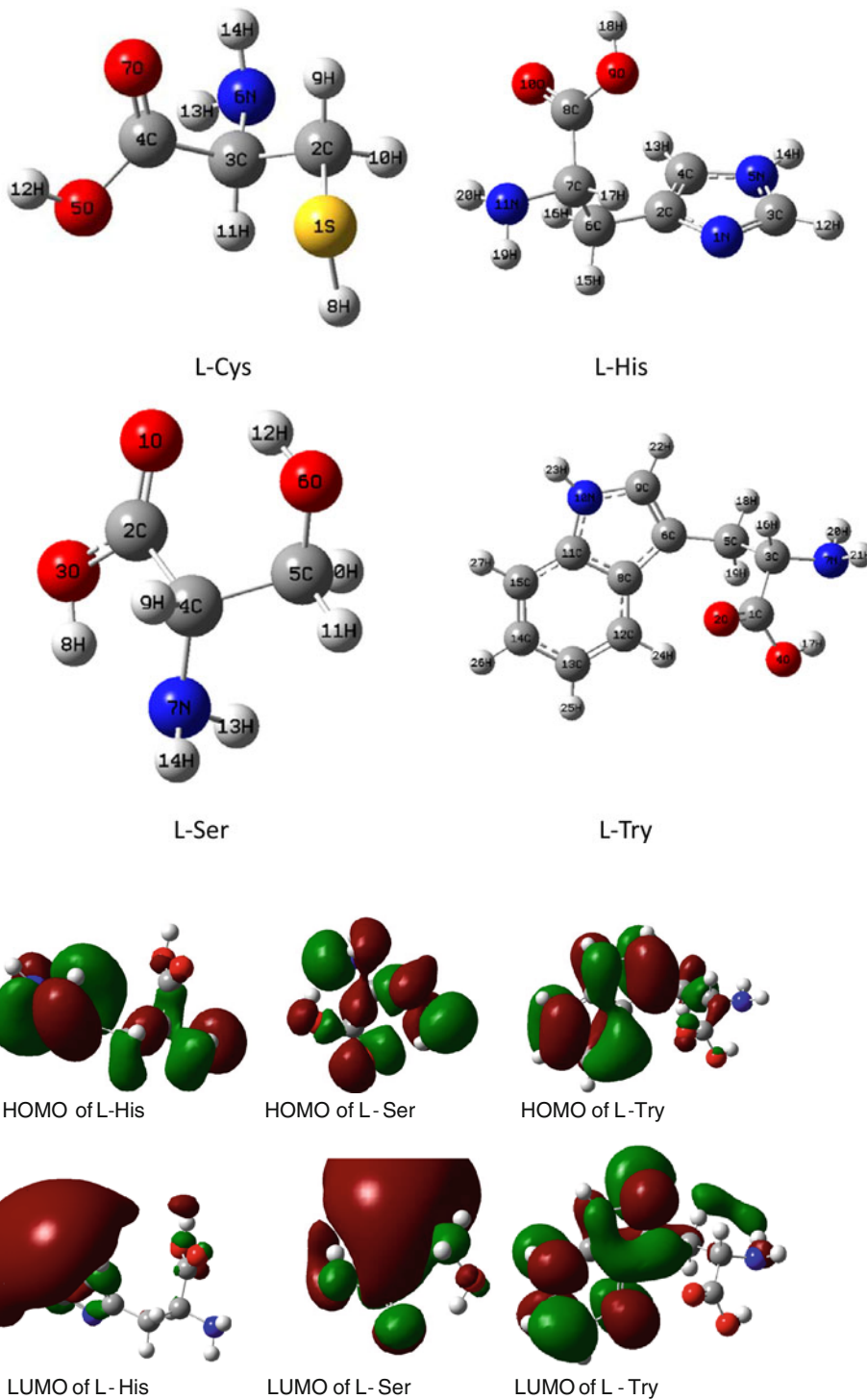


Fig. 5 The frontier molecular orbital density distribution of four amino acid compounds

Table 5. Additionally, the orbital density distributions of E_{HOMO} and E_{LUMO} for amino acid compounds were shown in Fig. 5.

According to the frontier orbital theory, E_{HOMO} is often associated with the electron donating ability of a molecule. High values of E_{HOMO} indicate a tendency of the molecule

to donate electrons to appropriate acceptor molecules with low-energy, empty electron orbital. Similarly, E_{LUMO} represents the ability of the molecule to accept electrons. The lower the values of E_{LUMO} , the more probable it is that the molecule would accept electrons [41]. ΔE , the difference of E_{LUMO} and E_{HOMO} , is another important factor that should

Table 5 Calculated quantum chemical parameters of amino acid compounds

| Molecules | Total energy (a.u.) | HOMO (eV) | LUMO (eV) | ΔE (eV) | μ | ΔN |
|-----------|---------------------|-----------|-----------|-----------------|--------|------------|
| L-Cys | −722.089 | −6.830 | −0.517 | 6.313 | 2.2542 | 0.5269 |
| L-His | −548.967 | −6.367 | −0.272 | 6.095 | 3.7935 | 0.5782 |
| L-Try | −686.602 | −5.687 | −0.626 | 5.061 | 5.6402 | 0.7594 |
| L-Ser | −399.119 | −7.456 | −0.871 | 6.585 | 5.0449 | 0.4307 |

be considered. It has been reported that low values of ΔE will provide good inhibition efficiency, because the energy for removing an electron from the last occupied orbital will be low [42].

In Table 5, the values of E_{HOMO} of four amino acid compounds increased in the following order: L-Try > L-His > L-Cys > L-Ser. The values of ΔE decreased in the following order: L-Try < L-His < L-Cys < L-Ser. The sequences of E_{HOMO} and ΔE support the results obtained from the electrochemical measurements. The inhibition efficiency increased with increase in the E_{HOMO} and decrease in ΔE . L-Try has the highest E_{HOMO} and the lowest ΔE among these four amino acid compounds. Therefore, L-Try has the strongest interaction with iron surface and the best inhibition effect. However, it can be seen in Table 5, there are no obvious linear correlation between E_{LUMO} , μ and inhibition efficiency. Similar observations have been reported in some previous literature [43, 44].

Table 6 Calculated Mulliken atomic charges and Fukui functions for amino acid compounds

| Molecules | Atoms | f_k^+ | f_k^- | f_k^0 |
|-----------|-------|---------|---------|---------|
| L-Cys | S1 | 0.050 | 0.469 | 0.260 |
| | C4 | 0.257 | −0.011 | 0.123 |
| | O5 | 0.115 | 0.025 | 0.070 |
| | O7 | 0.216 | 0.067 | 0.142 |
| L-His | C3 | 0.033 | 0.066 | 0.050 |
| | C8 | 0.255 | −0.012 | 0.122 |
| | O9 | 0.113 | 0.020 | 0.066 |
| | O10 | 0.210 | 0.050 | 0.130 |
| | N11 | −0.001 | 0.210 | 0.104 |
| L-Ser | O1 | 0.199 | 0.135 | 0.167 |
| | C2 | 0.245 | 0.053 | 0.149 |
| | O3 | 0.118 | 0.071 | 0.095 |
| | O6 | 0.047 | 0.243 | 0.145 |
| | N7 | −0.026 | 0.100 | 0.037 |
| L-Try | C6 | 0.031 | 0.077 | 0.054 |
| | C9 | 0.103 | 0.071 | 0.087 |
| | N10 | 0.014 | 0.056 | 0.035 |
| | C12 | 0.100 | 0.061 | 0.080 |
| | C14 | 0.046 | 0.041 | 0.043 |
| | C15 | 0.096 | 0.053 | 0.074 |

The number of electrons transferred (ΔN) from the inhibitor molecule to the metallic atom was also calculated using the following equation:

$$\Delta N = \frac{\chi_{\text{Fe}} - \chi_{\text{Inh}}}{2(\eta_{\text{Fe}} + \eta_{\text{Inh}})} \quad (12)$$

where χ_{Fe} and χ_{Inh} represent the absolute electronegativity of iron and the inhibitor molecule, respectively; η_{Cu} and η_{inh} represent the absolute hardness of iron and the inhibitor molecule. These quantities are associated with electron affinity (A) and ionization potential (I) which are useful in their ability to help chemical behaviour [45].

$$\chi = \frac{I + A}{2} \quad (13)$$

$$\eta = \frac{I - A}{2} \quad (14)$$

I and A are related in turn to E_{HOMO} and E_{LUMO} as following equations:

$$I = -E_{\text{HOMO}} \quad (15)$$

$$A = -E_{\text{LUMO}} \quad (16)$$

Values of χ and η were calculated by using the values of I and A obtained from quantum chemical calculations. In order to calculate ΔN , a theoretical value for the electronegativity of bulk iron was used $\chi_{\text{Fe}} \approx 7$ eV, and a global hardness of $\eta_{\text{Fe}} \approx 0$, by assuming that for a metallic bulk $I = A$, because they are softer than the neutral metallic atoms. The values of ΔN for four amino acid compounds were also listed in Table 5.

According to Lukovits, if $\Delta N < 3.6$, the inhibition efficiency increased with increasing electron donating ability at the metal surface [46]. It can be inferred from the calculation results that inhibitors investigated in this study were donors of electrons, and the iron surface was the acceptor. Order of ΔN is as follow: L-Try > L-His > L-Cys > L-Ser, which is in accordance with the change trends of E_{HOMO} and inhibition efficiency. The highest inhibition efficiency of L-Try can be attributed to the strongest coordinate bonds formed between the lone electron pairs of heterocyclic atom/ π electrons of indole ring and the vacant d-orbitals of the metal surface.

The local reactivity was analyzed by means of the Fukui Indices. Fukui functions are a qualitative way of measuring

and displaying the reactivity of a molecule [47]. The molecule sites with large values of f_k^+ are the sites where the molecule will receive charge, when attacked by a nucleophilic reagents, and the molecule sites with large values of f_k^- are the preferred sites where the molecule will donate charge when attacked by an electrophilic reagent [48]. The values of Fukui functions for a nucleophilic and electrophilic attack were shown in Table 6 for the four amino acid compounds, in which only the largest values were presented. For nucleophilic attack, the most reactive site of L-Cys is on the C4, O5 and O7 atom, L-His is on the C8, O9 and O10 atom, L-Ser is on O1, C2 and O3 atom and L-Try is on C9, C12 and C15 atom. For electrophilic attack,

the most reactive site of L-Cys is on the S1 atom, L-His is on N11 atom, L-Ser is on O1, O2 and N7 atoms and L-Try is on C6, C9 and C12 atom of indole ring. The distributions of HOMO and LUMO on each inhibitor are basically consistent with the atoms that exhibit greatest values of f_k^- and f_k^+ , which demonstrate that these active atoms will play a significant role in the interaction with the iron surface.

Molecular dynamics simulation

The further information on the interaction between the inhibitor and the iron surface can be provided by the molecular dynamics simulations. Figure 6 shows the

Fig. 6 Equilibrium adsorption configurations of inhibitor molecules on Fe (1 1 0)

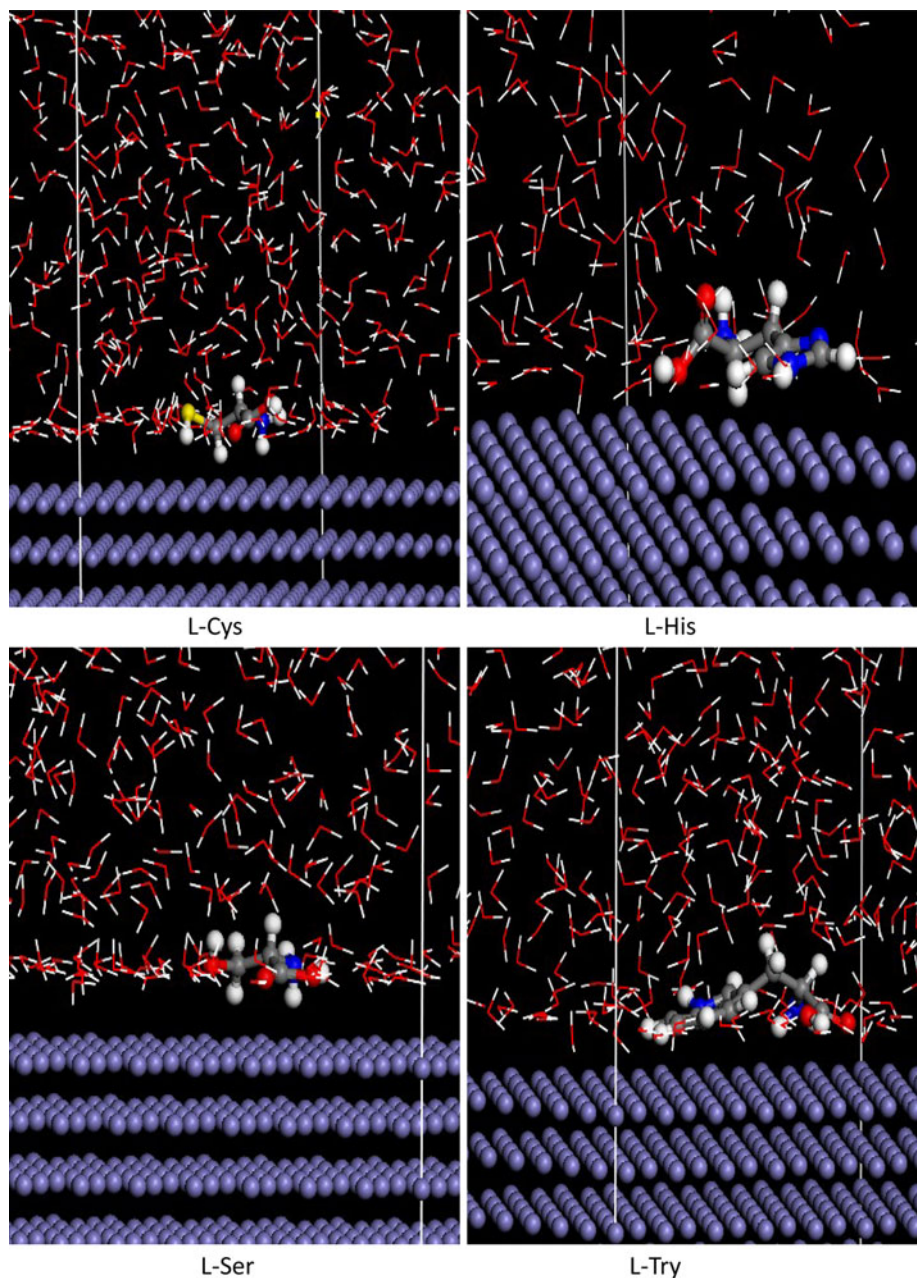


Table 7 Calculated interactional energy between inhibitor molecule and iron surface from molecular dynamics simulations

| Inhibitor | $E_{\text{interaction}}$ (kJ mol ⁻¹) | E_{binding} (kJ mol ⁻¹) |
|-----------|--|--|
| L-Cys | -275 | 275 |
| L-His | -289 | 289 |
| L-Try | -402 | 402 |
| L-Ser | -255 | 255 |

different adsorption equilibrium configurations of four amino acid compounds. Through the simulation process, each configuration changed greatly. By comparing the equilibrium configurations of four amino acid compounds adsorbed on Fe (1 1 0) surface, it can be conclude that L-Cys and L-Ser can be adsorbed on the iron surface through the heterocyclic atoms in their molecules, while L-His and L-Try can be adsorbed on the iron surface through not only the heterocyclic atoms but also the imidazole ring and the indole ring, respectively. Both interactions can make it possible for amino acid compounds to form coordinated bonds with iron surface, and form the compact film preventing the corrosive media to move to the metal surface.

The values of the interaction energy and the binding energy of the four amino acid compounds on iron surface were listed in Table 7. In all cases, the binding energy has a positive value. Generally, the binding energy increases, the more stable the inhibitor adsorbs on the metal surface, and the high inhibition efficiency. Based on the calculations, L-Ser presented the lowest binding energy value of 256 kJ mol⁻¹, followed by L-Cys with 275 kJ mol⁻¹ and L-His with 289 kJ mol⁻¹. Finally, L-Try displayed the highest value of 402 kJ mol⁻¹. L-His has the highest binding energy during the simulation process. A number of lone pair of electrons on the O and N atoms as well as the π -electron clouds on the indole ring can provide electrons to the unfilled 3d-orbitals of iron surface to form protective layer. High values of binding energy obtained with L-Try molecule explain its highest inhibition efficiency from the electrochemical measurements.

Summary and Conclusions

1. Tafel polarization and EIS technique were used to characterize the corrosion inhibition of mild steel in 1MHCl by the four amino acid compounds. The inhibition efficiency increased as follows, L-Ser < L-Cys < L-His < L-Try under the same experimental condition.
2. Calculations of the E_{HOMO} , ΔE and ΔN illuminate that the order of the inhibition efficiency of these inhibitors follows the sequence: L-Try > L-His > L-Cys > L-Ser,

and this result consists well with the experimental results.

3. The molecular dynamics simulation results show that these four amino acid compounds can absorb on the iron surface through the heteroatoms and heterocyclic ring in their structures.

Acknowledgement The authors are pleased to acknowledge the financial support provided by Specialized Research Fund for the Doctoral Program of Higher Education, China (No. 20093219120014) and NUST Research Funding, China (No. 2010ZYTS016).

References

1. Fouda AS, Mostafa HA, El-Abbasy HM (2010) J Appl Electrochem 40:163
2. Amin MA, Abd El Rehim SS, El-Naggar MM, Abdel-Fatah HTM (2010) J Mater Sci 44:6258. doi:[10.1007/s10853-009-3856-2](https://doi.org/10.1007/s10853-009-3856-2)
3. Abelev E, Sellberg J, Ramanarayanan TA, Bernasek SL (2010) J Mater Sci 44:6167. doi:[10.1007/s10853-009-3854-4](https://doi.org/10.1007/s10853-009-3854-4)
4. Shukla SK, Singh AK, Ahamed I, Quraishi MA (2009) Mater Lett 63:819
5. Shukla SK, Quraishi MA (2009) J Appl Electrochem 39:1517
6. Sinko J (2001) Prog Org Coat 42:267
7. Bothi Raja P, Sethuraman MG (2008) Mater Lett 62:1602
8. Ketsdzi A, Stathoulopoulou A, Demadis KD (2008) Desalination 223:487
9. Umores SA, Obot IB, Obi-Egbedi NO (2009) J Mater Sci 44:274. doi:[10.1007/s10853-008-3045-8](https://doi.org/10.1007/s10853-008-3045-8)
10. Lyon S (2004) Nature 427:406
11. Fu JJ, Li SN, Cao LH, Wang Y, Yan LH, Lu LD (2010) J Mater Sci 45:979. doi:[10.1007/s10853-009-4028-0](https://doi.org/10.1007/s10853-009-4028-0)
12. Saifi H, Bernard MC, Joiret S, Rahmouni K, Takenouti H, Talhi B (2010) Mater Chem Phys 120:661
13. Zhang DQ, Gao LX, Zhou GD (2005) J Appl Electrochem 35:1081
14. Zhang DQ, Cai QR, Gao LX, Lee KY (2008) Corros Sci 12:3615
15. Zerfaoui M, Oudda H, Hammouti B, Kertit S, Benkaddour M (2004) Prog Org Coat 51:134
16. Ashassi-Sorkhabi H, Ghasemi Z, Seifzadeh D (2005) Appl Surf Sci 249:408
17. Diab ASM, Abdel-Azzem M, Mandour H (2005) Bull Electrochem 21:97
18. Issa RM, Awad MK, Atlam FM (2008) Appl Surf Sci 255:2433
19. Avci G (2008) Colloids Surf A 317:730
20. Granero MFL, Matai PHLS, Aoki IV, Guedes IC (2009) J Appl Electrochem 39:1199
21. Behpour M, Ghoreishi SM, Gandomi-Niasar A, Soltani N, Salavati-Niasari M (2009) J Mater Sci 44:2444. doi:[10.1007/s10853-009-3309-y](https://doi.org/10.1007/s10853-009-3309-y)
22. Gece G (2008) Corros Sci 50:2981
23. Jamalizadeh E, Jafari AH, Hosseini SMA (2008) J Mol Struct 870:23
24. Lukovits I, Shaban A, Kálmán E (2005) Electrochim Acta 50:4128
25. Duda Y, Govea-Rueda R, Galicia M, Beltraén HI, Zamudio-Rivera LS (2005) J Phys Chem B 109:22674
26. Gómez B, Likhanova NV, Aguilar MAD, Olivares O, Hallen JM, Martínez-Magadán JM (2005) J Phys Chem A 109:8950
27. Zhang SG, Lei W, Xia MZ, Wang FY (2005) J Mol Struct 732:173

28. Tang YM, Chen Y, Yang WZ, Liu Y, Yin XS, Wang JT (2008) *J Appl Electrochem* 38:1553
29. Feng Y, Chen S, Guo W, Liu G, Ma H, Wu L (2007) *Appl Surf Sci* 253:8734
30. Khaled KF (2009) *J Solid State Electrochem* 13:1743
31. Khaled KF, Amin MA (2009) *Corros Sci* 51:1964
32. Khaled KF, Amin MA (2009) *J Appl Electrochem* 39:2553
33. Rodríguez-Valdez LM, Villamizar W, Casales M, González-Rodríguez JG, Martínez-Villafaña A, Martinez L, Glossman-Mitnik D (2006) *Corros Sci* 48:4053
34. Wang H, Wang X, Wang H, Wang L, Liu A (2007) *J Mol Model* 13:147
35. Xia S, Qiu M, Yu L, Liu F, Zhao H (2008) *Corros Sci* 50:2021
36. Khaled KF (2008) *Electrochim Acta* 53:3484
37. Oguzie EE, Li Y, Wang FH (2007) *Electrochim Acta* 53:909
38. Oguzie EE, Wang SG, Li Y, Wang FH (2008) *J Solid State Electrochem* 12:721
39. Gopi D, Govindaraju KM, Kavitha L (2010) *J Appl Electrochem*. doi:[10.1007/s10800-010-0092-z](https://doi.org/10.1007/s10800-010-0092-z)
40. Prabhu RA, Venkatesha TV, Shanbhag AV, Praveen BM, Kulkarni GM, Kalkhambkar RG (2008) *Mater Chem Phys* 108:283
41. Şahin M, Gece G, Karcı F, Bilgiç S (2008) *J Appl Electrochem* 38:809
42. Gece G, Bilgiç S (2009) *Corros Sci* 51:1876
43. Özcan M, Dehri I, Erbil M (2004) *Appl Surf Sci* 236:155
44. Li W, He Q, Pei C, Hou B (2007) *Electrochim Acta* 52:6386
45. Obot IB, Obi-Egbedi NO (2010) *Corros Sci* 52:198
46. Larabi L, Benali O, Mekelleche SM, Harek Y (2006) *Appl Surf Sci* 253:1371
47. Cruz J, Martínez-Aguilera LMR, Salcedo R, Castro M (2001) *Int J Quantum Chem* 85:546
48. Khaled KF, Amin MA (2009) *Corros Sci* 51:2098